In vitro characterization of genetically expressed absorbing proteins using photoacoustic spectroscopy

Jan Laufer,[1,4,5] Amit Jathoul,[2,3,5] Martin Pule,[2,3,6] and Paul Beard[1,3,5,*]

[1]*Department of Medical Physics and Bioengineering, University College London, Gower Street, London WC1E 6BT, UK*

[2]*Department of Haematology, Cancer Institute, University College London, 72 Huntley Street, London WC1E 6DD, UK*

[3]*Centre for Advanced Biomedical Imaging, Cancer Institute, University College London, 72 Huntley Street, London WC1E 6DD, UK*

[4]*Julius Wolff Institut, Charité – Universitätsmedizin Berlin, Augustenburger Platz 1, 13353 Berlin, Germany*

[5]*Contributed equally to this work*

[6]*Contributed equally to this work*

*paul.beard@ucl.ac.uk

Abstract: Genetically expressed fluorescent proteins have been shown to provide photoacoustic contrast. However, they can be limited by low photoacoustic generation efficiency and low optical absorption at red and near infrared wavelengths, thus limiting their usefulness in mammalian small animal models. In addition, many fluorescent proteins exhibit low photostability due to photobleaching and transient absorption effects. In this study, we explore these issues by synthesizing and characterizing a range of commonly used fluorescent proteins (dsRed, mCherry, mNeptune, mRaspberry, AQ143, E2 Crimson) and novel non-fluorescent chromoproteins (aeCP597 and cjBlue and a non-fluorescent mutant of E2 Crimson). The photoacoustic spectra, photoacoustic generation efficiency and photostability of each fluorescent protein and chromoprotein were measured. Compared to the fluorescent proteins, the chromoproteins were found to exhibit higher photoacoustic generation efficiency due to the absence of radiative relaxation and ground state depopulation, and significantly higher photostability. The feasibility of converting an existing fluorescent protein into a non-fluorescent chromoprotein via mutagenesis was also demonstrated. The chromoprotein mutant exhibited greater photoacoustic signal generation efficiency and better agreement between the photoacoustic and the specific extinction coefficient spectra than the original fluorescent protein. Lastly, the genetic expression of a chromoprotein in mammalian cells was demonstrated. This study suggests that chromoproteins may have potential for providing genetically encoded photoacoustic contrast.

©2013 Optical Society of America

OCIS codes: (110.5125) Photoacoustics; (300.0300) Spectroscopy; (000.1430) Biology and medicine.

References and links

1. S. R. Cherry, "In vivo molecular and genomic imaging: new challenges for imaging physics," Phys. Med. Biol. **49**(3), R13–R48 (2004).
2. Y. Yu, A. J. Annala, J. R. Barrio, T. Toyokuni, N. Satyamurthy, M. Namavari, S. R. Cherry, M. E. Phelps, H. R. Herschman, and S. S. Gambhir, "Quantification of target gene expression by imaging reporter gene expression in living animals," Nat. Med. **6**(8), 933–937 (2000).
3. P. Beard, "Biomedical photoacoustic imaging," Interface Focus **1**(4), 602–631 (2011).
4. A. Krumholz, S. J. Vanvickle-Chavez, J. Yao, T. P. Fleming, W. E. Gillanders, and L. V. Wang, "Photoacoustic microscopy of tyrosinase reporter gene in vivo," J. Biomed. Opt. **16**(8), 080503 (2011).
5. J. Laufer, A. Jathoul, P. Johnson, E. Zhang, M. Lythgoe, R. B. Pedley, M. Pule, and P. Beard, "In vivo photoacoustic imaging of tyrosinase expressing tumours in mice," Proc. SPIE **8223**, 82230M, 82230M-5 (2012).

6. L. Li, R. J. Zemp, G. Lungu, G. Stoica, and L. V. Wang, "Photoacoustic imaging of lacZ gene expression in vivo," J. Biomed. Opt. **12**(2), 020504 (2007).
7. X. Cai, L. Li, A. Krumholz, Z. Guo, T. N. Erpelding, C. Zhang, Y. Zhang, Y. Xia, and L. V. Wang, "Multi-scale molecular photoacoustic tomography of gene expression," PLoS ONE **7**(8), e43999 (2012).
8. R. L. Strack, B. Hein, D. Bhattacharyya, S. W. Hell, R. J. Keenan, and B. S. Glick, "A rapidly maturing far-red derivative of DsRed-Express2 for whole-cell labeling," Biochemistry **48**(35), 8279–8281 (2009).
9. M. R. Soboleski, J. Oaks, and W. P. Halford, "Green fluorescent protein is a quantitative reporter of gene expression in individual eukaryotic cells," FASEB J. **19**(3), 440–442 (2005).
10. D. Razansky, M. Distel, C. Vinegoni, R. Ma, N. Perrimon, R. W. Köster, and V. Ntziachristos, "Multispectral opto-acoustic tomography of deep-seated fluorescent proteins in vivo," Nat. Photonics **3**(7), 412–417 (2009).
11. G. S. Filonov, K. D. Piatkevich, L.-M. Ting, J. Zhang, K. Kim, and V. V. Verkhusha, "Bright and stable near-infrared fluorescent protein for in vivo imaging," Nat. Biotechnol. **29**(8), 757–761 (2011).
12. G. S. Filonov, A. Krumholz, J. Xia, J. Yao, L. V. Wang, and V. V. Verkhusha, "Deep-tissue photoacoustic tomography of a genetically encoded near-infrared fluorescent probe - supporting information," Angew. Chem. **124**(6), 1477–1480 (2012).
13. J. Hendrix, C. Flors, P. Dedecker, J. Hofkens, and Y. Engelborghs, "Dark states in monomeric red fluorescent proteins studied by fluorescence correlation and single molecule spectroscopy," Biophys. J. **94**(10), 4103–4113 (2008).
14. C. Blum and V. Subramaniam, "Single-molecule spectroscopy of fluorescent proteins," Anal. Bioanal. Chem. **393**(2), 527–541 (2009).
15. D. Stoner-Ma, A. A. Jaye, P. Matousek, M. Towrie, S. R. Meech, and P. J. Tonge, "Observation of excited-state proton transfer in green fluorescent protein using ultrafast vibrational spectroscopy," J. Am. Chem. Soc. **127**(9), 2864–2865 (2005).
16. G. S. Baird, D. A. Zacharias, and R. Y. Tsien, "Biochemistry, mutagenesis, and oligomerization of DsRed, a red fluorescent protein from coral," Proc. Natl. Acad. Sci. U.S.A. **97**(22), 11984–11989 (2000).
17. N. C. Shaner, R. E. Campbell, P. A. Steinbach, B. N. Giepmans, A. E. Palmer, and R. Y. Tsien, "Improved monomeric red, orange and yellow fluorescent proteins derived from Discosoma sp. red fluorescent protein," Nat. Biotechnol. **22**(12), 1567–1572 (2004).
18. M. Z. Lin, M. R. McKeown, H.-L. Ng, T. A. Aguilera, N. C. Shaner, R. E. Campbell, S. R. Adams, L. A. Gross, W. Ma, T. Alber, and R. Y. Tsien, "Autofluorescent proteins with excitation in the optical window for intravital imaging in mammals," Chem. Biol. **16**(11), 1169–1179 (2009).
19. L. Wang, W. C. Jackson, P. A. Steinbach, and R. Y. Tsien, "Evolution of new nonantibody proteins via iterative somatic hypermutation," Proc. Natl. Acad. Sci. U.S.A. **101**(48), 16745–16749 (2004).
20. M. A. Shkrob, Y. G. Yanushevich, D. M. Chudakov, N. G. Gurskaya, Y. A. Labas, S. Y. Poponov, N. N. Mudrik, S. Lukyanov, and K. A. Lukyanov, "Far-red fluorescent proteins evolved from a blue chromoprotein from Actinia equina," Biochem. J. **392**(3), 649–654 (2005).
21. W. P. Stemmer, A. Crameri, K. D. Ha, T. M. Brennan, and H. L. Heyneker, "Single-step assembly of a gene and entire plasmid from large numbers of oligodeoxyribonucleotides," Gene **164**(1), 49–53 (1995).
22. A. N. Warrens, M. D. Jones, and R. I. Lechler, "Splicing by overlap extension by PCR using asymmetric amplification: an improved technique for the generation of hybrid proteins of immunological interest," Gene **186**(1), 29–35 (1997).
23. B. J. Bevis and B. S. Glick, "Rapidly maturing variants of the Discosoma red fluorescent protein (DsRed)," Nat. Biotechnol. **20**(1), 83–87 (2002).
24. D. Shcherbo, I. I. Shemiakina, A. V. Ryabova, K. E. Luker, B. T. Schmidt, E. A. Souslova, T. V. Gorodnicheva, L. Strukova, K. M. Shidlovskiy, O. V. Britanova, A. G. Zaraisky, K. A. Lukyanov, V. B. Loschenov, G. D. Luker, and D. M. Chudakov, "Near-infrared fluorescent proteins," Nat. Methods **7**(10), 827–829 (2010).
25. M. C. Y. Chan, S. Karasawa, H. Mizuno, I. Bosanac, D. Ho, G. G. Privé, A. Miyawaki, and M. Ikura, "Structural characterization of a blue chromoprotein and its yellow mutant from the sea anemone Cnidopus japonicus," J. Biol. Chem. **281**(49), 37813–37819 (2006).
26. M. E. Bulina, D. M. Chudakov, N. N. Mudrik, and K. A. Lukyanov, "Interconversion of Anthozoa GFP-like fluorescent and non-fluorescent proteins by mutagenesis," BMC Biochem. **3**(1), 7 (2002).
27. E. Zhang, J. Laufer, and P. Beard, "Backward-mode multiwavelength photoacoustic scanner using a planar Fabry-Perot polymer film ultrasound sensor for high-resolution three-dimensional imaging of biological tissues," Appl. Opt. **47**(4), 561–577 (2008).
28. C. Ruckebusch, M. Sliwa, P. Pernot, A. de Juan, and R. Tauler, "Comprehensive data analysis of femtosecond transient absorption spectra: A review," J. Photochem. Photobiol. Photochem. Rev. **13**(1), 1–27 (2012).
29. M. Cotlet, J. Hofkens, S. Habuchi, G. Dirix, M. Van Guyse, J. Michiels, J. Vanderleyden, and F. C. De Schryver, "Identification of different emitting species in the red fluorescent protein DsRed by means of ensemble and single-molecule spectroscopy," Proc. Natl. Acad. Sci. U.S.A. **98**(25), 14398–14403 (2001).
30. W. Min, S. Lu, S. Chong, R. Roy, G. R. Holtom, and X. S. Xie, "Imaging chromophores with undetectable fluorescence by stimulated emission microscopy," Nature **461**(7267), 1105–1109 (2009).
31. J. W. Lichtman and J. A. Conchello, "Fluorescence microscopy," Nat. Methods **2**(12), 910–919 (2005).
32. J. W. Borst and A. J. W. G. Visser, "Fluorescence lifetime imaging microscopy in life sciences," Meas. Sci. Technol. **21**(10), 102002 (2010).
33. N. C. Shaner, M. Z. Lin, M. R. McKeown, P. A. Steinbach, K. L. Hazelwood, M. W. Davidson, and R. Y. Tsien, "Improving the photostability of bright monomeric orange and red fluorescent proteins," Nat. Methods **5**(6), 545–551 (2008).

34. K. D. Piatkevich, E. N. Efremenko, V. V. Verkhusha, and S. D. Varfolomeev, "Red fluorescent proteins and their properties," Russ. Chem. Rev. **79**(3), 243–258 (2010).
35. B. T. Cox, S. R. Arridge, and P. C. Beard, "Estimating chromophore distributions from multiwavelength photoacoustic images," J. Opt. Soc. Am. A **26**(2), 443–455 (2009).
36. J. Laufer, B. Cox, E. Zhang, and P. Beard, "Quantitative determination of chromophore concentrations from 2D photoacoustic images using a nonlinear model-based inversion scheme," Appl. Opt. **49**(8), 1219–1233 (2010).
37. R. Y. Tsien, "The green fluorescent protein," Annu. Rev. Biochem. **67**(1), 509–544 (1998).

1. Introduction

Reporter gene methods provide the opportunity to image biological events such as gene expression, signaling pathways, cell proliferation, and apoptosis [1,2]. In photoacoustic imaging [3], two approaches have been explored. One approach involves the genetic expression of enzymes which form an optically absorbing chromophore that provides the source of photoacoustic contrast. For example, tyrosinase converts tyrosine into eumelanin, an endogenous tissue chromophore that absorbs in the visible and near-infrared part of the spectrum. This has been used to visualize otherwise transparent tumor cells using photoacoustic imaging *in vivo* [4,5]. Another enzymatic approach is the genetic expression of β-galactosidase, an Escherichia coli enzyme involved in the metabolism of lactose, from the *lacZ* gene. However, this has the disadvantage that it requires the local injection of an exogenous chromogenic substance (X-gal) into the region of interest in order to visualize the presence of β-galactosidase [6,7]. The second approach relies upon the genetic expression of fluorescent proteins. Photoacoustic contrast is then achieved by exciting at a wavelength that lies within the absorption band of the protein. This approach is attractive because there are already a number of fluorescent proteins which have been engineered to be tolerated even at high concentrations and do not interfere with cell function and metabolism [8]. In addition, unlike genetically expressed enzymes, fluorescent proteins provide a 1:1 mapping to the expression level of the protein of interest [9] and their expression is not confounded by substrate availability and enzyme kinetics and hence more reliably reports the marker gene. Furthermore, the slow accumulation and clearance of enzyme metabolized pigment means that fluorescent proteins are better suited as genetically encodable reporters of transcription and cellular signaling. Genetically expressed fluorescent proteins have been visualized using photoacoustic imaging in the relatively transparent zebrafish and small scale Drosophila (fruitfly) pupa [10]. However, their use as photoacoustic genetic reporters in mammalian tissues is limited by a paucity of red-shifted variants, the latter being required to avoid strong absorption by hemoglobin below 650 nm. A rare exception is the near-infrared fluorescent protein, iRFP [11,12], which has an absorption peak at 680 nm. However its biosynthesis requires biliverdin, a by-product of the heme breakdown. In tissues where biliverdin is not readily available, systemic administration may be required to facilitate iRFP expression. A further consideration is that relatively little is known about the response of fluorescent proteins to the high peak power laser pulses typically used to generate photoacoustic signals. For example, many fluorescent proteins lack photostability, which can manifest itself as dark states [13], blinking [14], transient absorption [15], and photobleaching [8] and these effects may also compromise the photoacoustic stability and other characteristics of the protein. Not least, the photoacoustic generation efficiency of fluorescent proteins is likely to be reduced by radiative relaxation and ground state depopulation.

In this study, we address the above issues by synthesizing a range of commonly used purified fluorescent proteins and measuring their photoacoustic spectra, photoacoustic generation efficiency and photostability. In addition, as a potential alternative to fluorescent proteins, we synthesized and characterized a number of non-fluorescent purified chromoproteins and demonstrated chromoprotein expression in mammalian cells.

2. Methods

A number of fluorescent proteins and non-fluorescent chromoproteins were synthesized and their optical and photoacoustic properties measured. Six commonly used genetically expressed fluorescent proteins (dsRed, mCherry, mNeptune, mRaspberry, AQ143, E2

Crimson), two novel non-fluorescent chromoproteins (aeCP597 and cjBlue) and a non-fluorescent mutant of E2 Crimson were synthesised. The optical absorption spectrum, photoacoustic spectrum and photostability of each protein were then measured.

2.1 Synthesis of fluorescent proteins and chromoproteins

The genes encoding the fluorescent proteins dsRed [16], mCherry [17], mNeptune [18], mRaspberry [19], AQ143 [20], and E2 Crimson [8] and the chromoproteins aeCP597 [20] and cjBlue were synthesized in four stages.

First, a gene encoding for a fluorescent protein or chromoprotein is assembled using commercially available oligonucleotide fragments (short, single stranded DNA molecules). This method relies on polymerase amplification of larger DNA fragments from short oligonucleotides and subsequent generation of entire gene products by polymerase chain reaction of generated fragments [21]. To create site-directed and semi-random site-directed single or double mutants, genes were amplified using overlapping mutated primers by splicing by overlap extension polymerase chain reaction [22].

Second, the fragment containing the gene is excised using enzymes (NcoI, NotI) and incorporated into a bacterial expression vector (pGex 6p 2, GE Life Sciences, Sweden), a process called subcloning. The new gene not only encodes the protein of interest but also a glutathione-S-transferase (GST)-tag, which is later used for protein purification.

Third, the gene is introduced into transformation competent bacteria by heat shock (*Escherichia Coli* DH5α, New England Biolabs, USA) where the bacterial expression vector facilitates the protein expression. The use of bacterial cells instead of mammalian cells has the advantage that the rapid bacterial growth results in the expression of large quantities of proteins in a short space of time. Induction of protein expression results in a fusion protein of the fluorescent or chromoprotein and the GST-tag. Bacterial colonies were screened by lifting them onto nitrocellulose membranes. By imaging their color and fluorescence separately using a camera (Nikon 550D, Japan), absorbing, non-fluorescent colonies were selected. The expression of fluorescent proteins or chromoproteins was confirmed by DNA sequencing. To produce bacterial over-expression, single colonies expressing clones were inoculated into 5 ml Luria-Bertoni (LB) medium with 100 μg/ml carbenicillin and cultured for 16 h at 37 °C. 1 ml of this culture was subsequently inoculated into 20 ml LB medium and cultured overnight. The resultant culture was inoculated into 200 ml medium and grown to an optical density (600 nm) of 0.6-0.7 units. Protein expression was induced by the addition of 1mM isopropyl β-D-1-thiogalactopyranoside (IPTG) and shaking incubation at 37°C for 4-6 hours or at 21°C overnight.

Fourth, fusion proteins were purified by exploiting the high affinity of the GST-tag with glutathione. After centrifugation of the bacteria suspension at 4600 rpm for 15 min, the pellet of compacted bacteria was re-suspended in B-PER bacterial lysis solution. The fusion proteins were purified using glutathione resin according to manufacturer's instructions (Pierce Biotechnology Inc., USA). Protein concentrations were measured using the bicinchoninic acid (BCA) protein quantification kit (Pierce Biotechnology Inc., USA). This finally provided samples of purified proteins dissolved in distilled water (50 – 100 μl volume) which were then characterized in terms of their optical and photoacoustic properties.

Absorption spectra of these samples were measured using spectrophotometers (Varioskan Flash or NanoDrop, Thermo Scientific, USA). For protein concentration normalization purposes, literature values of extinction coefficients were used to confirm the results of BCA assays (Table 1).

Table 1. Reported properties of selected fluorescent proteins and chromoproteins (italics).

Protein	Absorbance maximum, λ_{max} [nm]	Molar extinction coefficient [$M^{-1}cm^{-1}$]	Quantum efficiency	Reference
dsRed	558	52 000	0.68	[23]
mCherry	587	72 000	0.22	[17]
mRaspberry	598	86 000	0.15	[19]
mNeptune	600	67 000	0.20	[18]
AQ143	595	90 000	0.04	[20]
E2 Crimson	605, 611	126 000	0.23	[8,24]
aeCP597	597	110 000	-	[20]
cjBlue	610	66 700	-	[25]

2.2 Synthesis of non-fluorescent mutants of E2 Crimson

A disadvantage of fluorescent proteins is that they exhibit reduced photoacoustic generation efficiency because a proportion of the absorbed optical energy is converted to a fluorescent emission rather than heat. It would therefore be desirable if the fluorescence could be suppressed by genetic modification to enhance thermalization and thus increase the efficiency of the photoacoustic signal generation. E2 Crimson is a promising candidate for such modification for two reasons. First, it has been iteratively engineered from dsRed [8] for high expression and low toxicity in mammalian cells and far red excitation and emission (611 nm / 646 nm). Second, it has been shown that one mutation of dsRed removes its fluorescence property [26]. It is therefore possible that a similar modification of E2 Crimson can create a non-fluorescent protein with favorable biocompatibility but red-shifted absorbance compared to dsRed. To investigate this, the amino acid Ser 146 was semi-randomly mutated. The resultant mutants S146A, S146C, S146G and S146N were found to have maintained their absorbance properties but had markedly reduced fluorescence compared to E2 Crimson. From these mutants, S146A, referred to in this paper as E2 Crimson NF (non-fluorescent), was selected. Its fluorescence was found to be more than one order of magnitude lower than that of E2 Crimson and its absorbance maximum was $\lambda_{max} = 583$ nm and thus blue-shifted compared to E2 Crimson but still red-shifted compared to dsRed. Using the purification methods described in section 2.1, samples of E2 Crimson NF in distilled water were prepared for measurements of their optical and photoacoustic characteristics.

2.3 Transduction of mammalian cells to express chromoproteins

The highly engineered nature of the fluorescent proteins in Table 1 allows them to be expressed with high efficiency and low toxicity in mammalian cells. By contrast, the expression of chromoproteins in mammalian cells is much less well established. To explore the potential for chromoprotein expression in mammalian cells, the genes encoding aeCP597 and cjBlue were each sub-cloned into a mammalian retroviral vector SFG as a NcoI / MluI fragment. The retroviral vectors also contained an internal ribosome entry site (IRES), which was followed by a truncated gene encoding a human CD34 cell surface protein. CD34 was used at a later stage as a marker to attach fluorescent labels and to allow cell sorting. The retrovirus encoding the two chromoproteins and the darkened E2 Crimson was prepared by triple transfection of 293T cells with the retroviral vector and the genes that encode envelope proteins (gag-pol and RD114) using GeneJuice (Novagen EMD Biosciences Inc., USA). The

retrovirus was then used to incorporate the retroviral gene into the chromosome of human leukemia cells (K562), a process referred to as transduction. This involved incubating 250 μl virus on retronectin (Clontech, CA, USA) coated non-tissue culture treated 24-well plates for 15 min at room temperature and subsequent removal of virus, addition of 1.5×10^5 K562 cells, addition of a further 1 ml of virus and centrifugation at 1000 x *g* for 40 min before incubation at 37°C. Cells were cultured in Iscove's Modified Dulbecco's Medium supplemented with 10% foetal bovine serum and glutaMAX (Life Technologies Corp., CA, USA). The translation of the introduced genes resulted in the co-expression of the chromoproteins and CD34. Staining of CD34 tag using a fluorescent allophycocyanin-conjugated mouse anti-human CD34 antibody (BD Biosciences, USA) was used to analyse expression levels by fluorescence activated cell sorting (FACS) (Cyan Analyser Instrument, Beckman Coulter, USA). The CD34 tag also allows the selection of K562 cells with high expression levels using clinical grade magnetic selection columns (Miltenyi Biotec, Germany).

2.4 Experimental set-up

Samples of the purified fluorescent proteins and chromoproteins were characterized using the experimental set-up shown in Fig. 1. A wavelength tuneable optical parametric oscillator (OPO) laser system (Newport Spectra Physics / GWU GmbH) provided excitation pulses of 7 ns duration between 450 nm and 680 nm at a pulse repetition frequency of 50Hz. The output of the OPO laser system was coupled into a multimode fused silica fiber of 1.5mm diameter for mode scrambling, which produced a Gaussian far-field output profile at the distal fiber end. The fiber output illuminated a sample holder with a fluence in the range 1.2 mJ cm^{-2} to 1.7 mJ cm^{-2} depending on the excitation wavelength. The sample holder consisted of a transparent polymethylmethacrylate (PMMA) sheet of 4mm thickness with a conical recess (3.4mm radius, 2mm height) that holds a sample volume of approximately 24 μl. The sample was covered with a transparent polyester film, the edges of which were sealed using glycerine to prevent drying of the sample during the measurement. The sample holder was placed in a shallow water bath to allow the propagation of photoacoustic waves, which were generated by the absorption of the excitation laser pulses, to a Fabry-Perot polymer film interferometer (FPI) that acts as an ultrasound sensor [27]. Its operation involves illuminating the sensor with the output of a wavelength-tuneable continuous-wave interrogation laser and detecting the intensity of the reflected light. By tuning the interrogation laser wavelength to the peak derivative of the FPI transfer function, an acoustically induced modulation in the optical thickness of the interferometer produces a change in the reflected intensity that is detected by a photodiode. The photoacoustic signals were recorded using a digitizing oscilloscope (Tektronix TDS5430) and downloaded to a PC. A small portion of the excitation light was directed to a spectrometer (USB2000, Ocean Optics) to measure the OPO wavelength. Another portion was directed to an integrating sphere with an in-built wavelength-calibrated photodiode which was used to obtain a measure of the incident pulse energy in order to normalize the photoacoustic signals. The calibrated photodiode output and photoacoustic signals were averaged over 30 laser pulses to improve SNR.
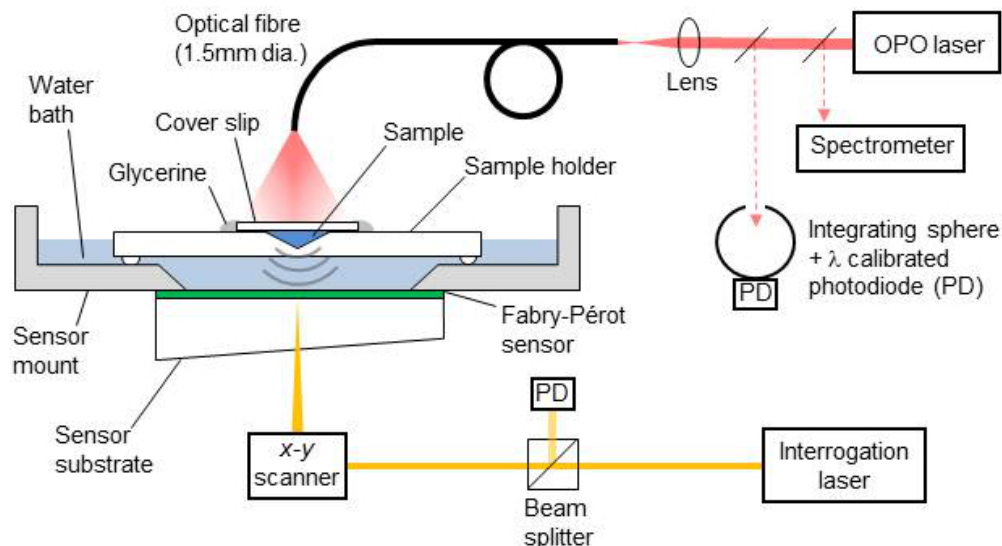
Fig. 1. Experimental set-up for measuring the photoacoustic signal amplitude in sample solutions of purified fluorescent proteins and chromoproteins.

To obtain the photoacoustic amplitude spectrum of a protein sample, the peak-to-peak values of photoacoustic signals generated at excitation wavelengths between 450 nm and 680 nm in 10 nm steps were recorded. To correct for the background absorption of the sample holder, the sample was replaced by distilled water and the photoacoustic amplitude spectrum measured in the same way and subtracted from the photoacoustic spectrum of the protein sample. For each protein species, amplitude spectra were measured in nine nominally identical samples. The protein concentrations of the solutions ranged from 20 to 80 μM. Photoacoustic amplitude spectra were also measured in phosphate-buffered saline suspensions of both the normal type (NT) K562 cells and those expressing aeCP597. The shape of the measured photoacoustic spectra was then compared to those of purified proteins measured using optical transmission spectroscopy. To obtain a quantitative measure of their agreement, the coefficient of determination, r^2, was calculated from a linear regression through a plot formed by the two types of spectra.

Photobleaching was assessed by recording the photoacoustic signal amplitude as a function of the number of laser pulses. The excitation wavelength was chosen to coincide with the absorption peak of the protein sample. The incident fluence was approximately 1.7 mJ cm^{-2}. For each species of protein, photobleaching curves were obtained by averaging the measurements in three samples.

3. Results

3.1 Photoacoustic amplitude spectra of fluorescent proteins

Figure 2 shows the photoacoustic amplitude spectra (circles) measured in six solutions of purified fluorescent proteins and their corresponding specific extinction spectra (dashed line), i.e. mCherry (Fig. 2(a)), mRaspberry (Fig. 2(b)), E2 Crimson (Fig. 2(c)), mNeptune (Fig. 2(d)), AQ143 (Fig. 2(e)), and dsRed (Fig. 2(f)). The error bars represent the standard deviation of nine measurements. To allow a qualitative comparison of the shape of the amplitude spectrum and that of the specific extinction coefficient spectrum, the vertical scales of each graph were adjusted by visual inspection until a reasonable match between the two data types was achieved. The r^2 values ranged from 0.86 for mCherry to 0.03 for AQ143.
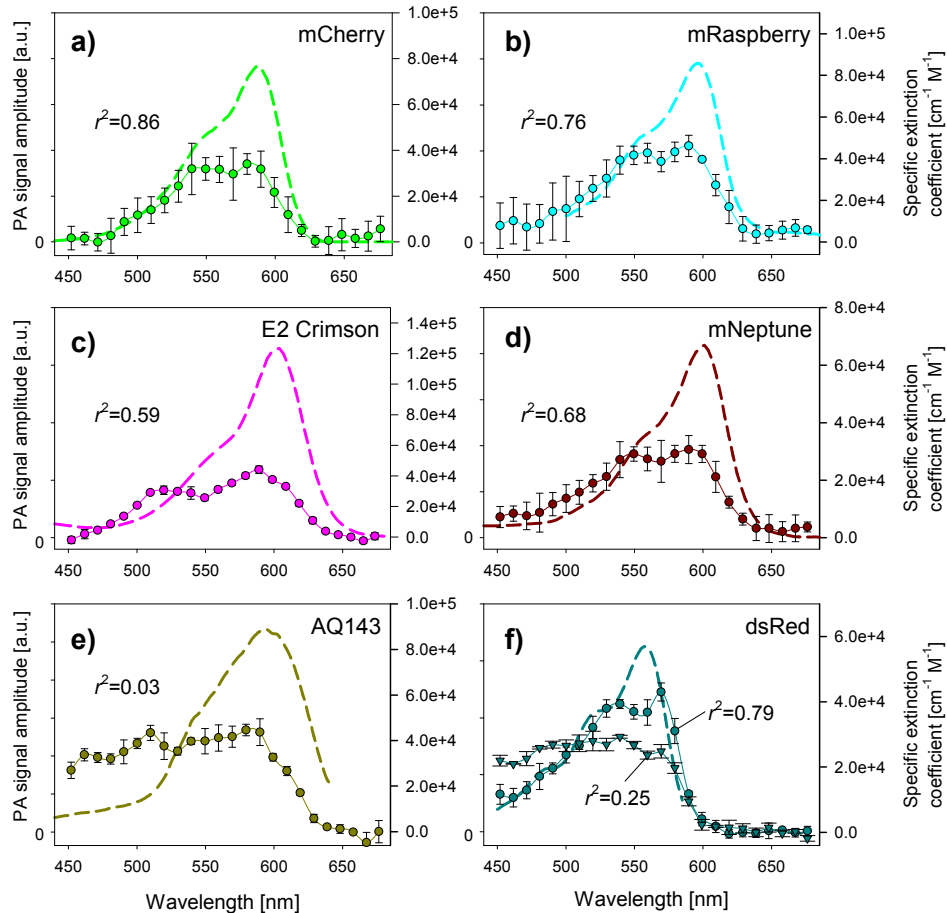
Fig. 2. Photoacoustic spectra (circles) of purified fluorescent protein solutions of (a) mCherry, (b) mRaspberry, (c) E2 Crimson, (d) mNeptune, (e) AQ143, and (f) dsRed in distilled water (triangles represent a repeat measurement after 24h) together with their specific extinction coefficient spectra (dashed lines). The error bars represent the standard deviation of the photoacoustic measurements.

Significant differences between the shapes of the specific extinction spectra and the corresponding photoacoustic amplitude spectra were observed for all fluorescent proteins, with AQ143 producing the poorest agreement. For all other fluorescent proteins, the differences are most noticeable at wavelengths around the absorption peak. These fluorescent proteins also exhibited a reduced photoacoustic amplitude at the peak absorption wavelength. The closest match between a photoacoustic spectrum and the specific extinction spectrum was observed in dsRed (Fig. 2(f)) where significant differences are only noticeable within a narrow region around 550 nm. However, dsRed also provided results that may suggest some form of molecular instability. A follow-up measurement on a sample from the same batch 24 h later produced a photoacoustic spectrum (also shown on Fig. 2(f)) with very different shape which was also in very poor agreement with the specific extinction spectrum. Figure 2 also confirms that most red or near-infrared fluorescent proteins exhibit relatively low optical absorption, and hence photoacoustic signal amplitude, for wavelengths longer than 620 nm. This is a major disadvantage for *in vivo* imaging applications in mammals where the absorption by haemoglobin is up to two orders of magnitude greater in the visible wavelength region compared to that in the near-infrared region.

3.2 Photoacoustic amplitude spectra of chromoproteins

Figure 3(a)-3(c) shows the photoacoustic amplitude spectra (circles) of the three chromoproteins (cjBlue, aeCP597, E2 Crimson NF) and their corresponding specific extinction spectra (dashed lines). The error bars represent the standard deviation of the measurements. The shape of the photoacoustic amplitude spectra are generally in good qualitative agreement with the specific extinction spectra. In addition, their optical absorption extends further into the near-infrared wavelength region. For example, cjBlue (Fig. 3(a)) exhibits significant absorption at wavelengths up to 650 nm. Figure 3(c) shows that eliminating the fluorescence in E2 Crimson through genetic modifications resulted in a blue-shift of the absorption, and hence photoacoustic amplitude spectrum, with a maximum at 585 nm. The r^2 values ranged from 0.95 to 0.97 and are significantly greater than those observed for fluorescent proteins.
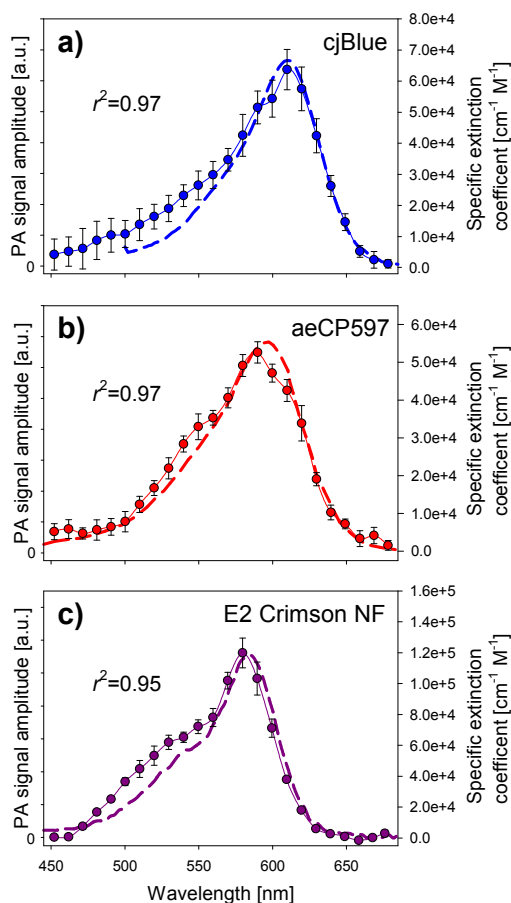

Fig. 3. Photoacoustic spectra (circles) of purified chromoprotein solutions of (a) cjBlue, (b) aeCP597, and (c) E2 Crimson NF in distilled water. The corresponding specific extinction coefficient spectra are shown as a dashed line. The error bars represent the standard deviation of the photoacoustic measurements.

3.3 Photoacoustic amplitude spectra normalized to the absorption coefficient

The amplitude spectra were divided by the peak absorption coefficient of the sample solutions as measured by the spectrophotometer. Normalizing for absorption in this way allowed for a direct comparison of the photoacoustic amplitude spectra of all proteins, and provides an indication of the photoacoustic generation efficiency of each protein species, i.e. how much of

the optical energy is thermalized and converted to pressure. Figure 4 shows the absorption normalized photoacoustic amplitude spectra of the chromoproteins E2 Crimson NF, aeCP597, and cjBlue, and the fluorescent proteins E2 Crimson, mNeptune, mRaspberry, and mCherry. The photoacoustic signal amplitude produced by the fluorescent proteins is less than half that observed in the chromoproteins, suggesting lower photoacoustic generation efficiency. Figure 4 clearly demonstrates that chromoproteins provide stronger photoacoustic signals than fluorescent proteins. In addition, the low photoacoustic signal amplitude observed in the fluorescent protein E2 Crimson around the absorption peak is not seen in its non-fluorescent counterpart E2 Crimson NF. The discrepancy between the photoacoustic and optical absorption spectra frequently seen in fluorescent proteins appears to have been eliminated.
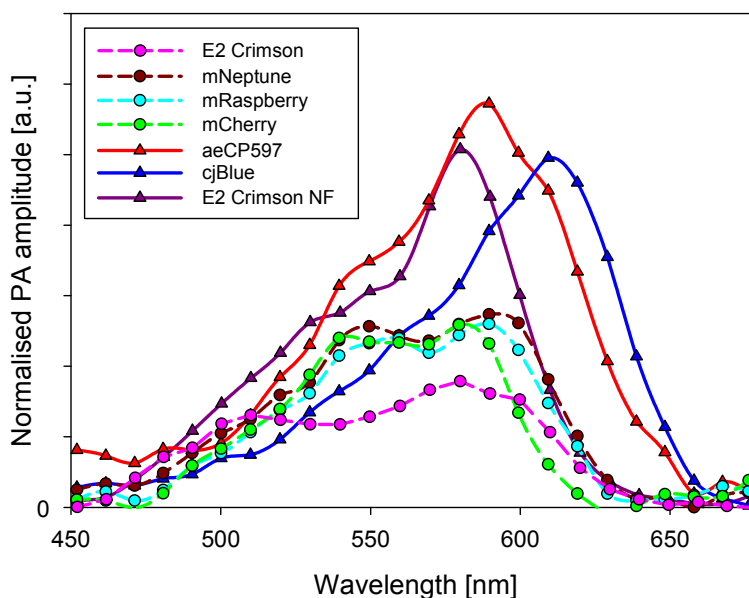

Fig. 4. Absorption-normalized photoacoustic spectra of fluorescent proteins (mNeptune, mRaspberry, mCherry, E2 Crimson) and chromoproteins (aeCP597, cjBlue, E2 Crimson NF).

3.4 Photobleaching

To assess photobleaching, each protein sample was irradiated with a train of excitation laser pulses at the 50Hz PRF of the excitation laser. The photoacoustic signal amplitude was recorded as a function of the number of incident laser pulses as shown in Fig. 5. Most of the fluorescent proteins exhibited an irreversible decrease in signal amplitude with increasing number of laser pulses. The most rapid decline in absorption was seen in mRaspberry, where the signal amplitude decreased by 60% after approximately 10000 pulses. In most other fluorescent proteins, the signal amplitude decreased by 50-30% within 35000 pulses. E2 Crimson FP was the exception and provided almost constant signal amplitude during the measurement. This is somewhat surprising since E2 Crimson has been shown to exhibit biphasic photobleaching in confocal microscopy [8] although the average radiant power was several orders of magnitude higher than that used in the current study which may explain the absence of photobleaching.

In contrast to the majority of fluorescent proteins, the chromoproteins showed only minor photobleaching. The photoacoustic signal amplitude measured in E2 Crimson NF was almost constant throughout the measurement, while that measured in cjBlue and aeCP597 decreased by 11% and 12%, respectively.
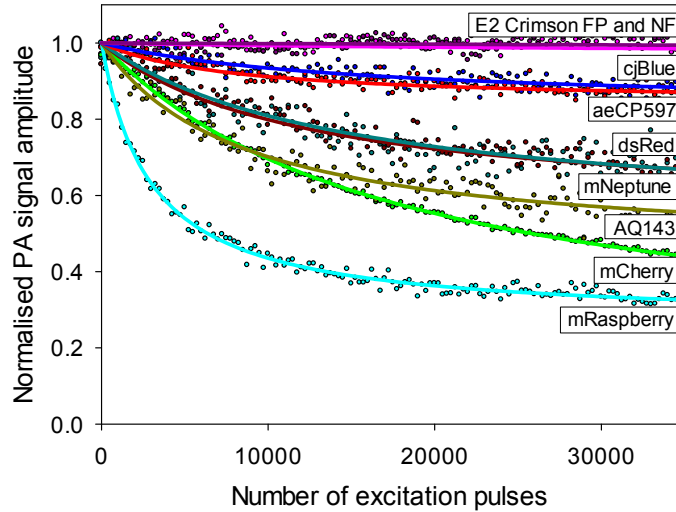
Fig. 5. Photobleaching of fluorescent proteins and chromoproteins under prolonged exposure to nanosecond laser pulses. The fluence at the sample ranged from 1.5 to 1.7 mJ cm^{-2}.

3.5 Photoacoustic amplitude spectra of chromoproteins expressed in human tumor cells

K562 cells were stably and homogeneously transduced to express cjBlue and aeCP597 as described in section 2.3. While the expression of cjBlue was confirmed using fluorescence activated flow cytometry, the expression level (and hence chromoprotein concentration) was too low for photoacoustic detection. aeCP597, by contrast was sufficiently well expressed to allow photoacoustic measurements. Figure 6(a) shows photoacoustic spectra detected in normal type (NT) and aeCP597 expressing human K562 tumor cells. In NT cells, the photoacoustic signal amplitude decreased with increasing wavelength. The shape of the spectrum results from optical absorption in other proteins and cell constituents and optical scattering by cellular components, such as cell membranes, vacuoles, and mitochondria. The photoacoustic amplitude spectrum of cells expressing aeCP597 shows significantly higher values between 560 nm and 630 nm than that measured in NT cells. The difference between these spectra is shown in Fig. 6(b) and is in good qualitative agreement with the specific extinction coefficient spectrum of aeCP597 shown in Fig. 3(b). The expression of aeCP597 was further confirmed by flow cytometry. Figure 7 shows cell count histograms as a function of the fluorescent intensity of allophycocyanin detected in NT cells and cells that were transduced to express aeCP597. Since allophycocyanin was bound to the co-expressed cell surface marker CD34, the fluorescent intensity is directly linked to the expression of aeCP597. Figure 7 shows that the expression level of CD34 is two orders of magnitude greater in the transduced cells compared to that of the normal type cells.
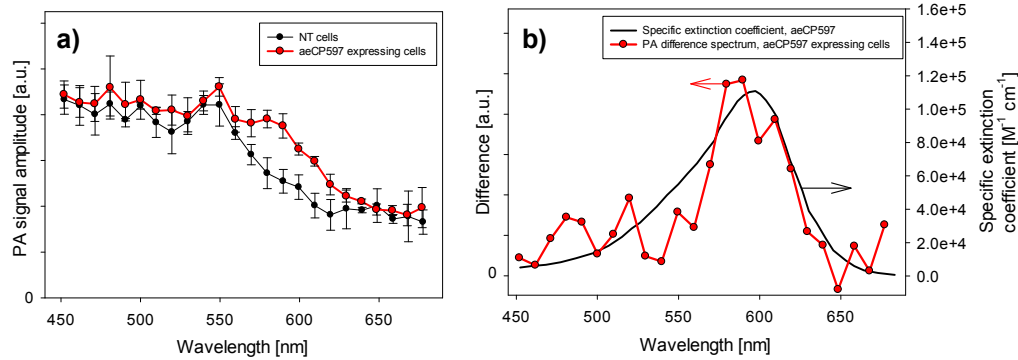
Fig. 6. (a) Photoacoustic amplitude spectra of normal type (NT) and aeCP597-expressing mammalian tumor cells (K562). (b) The difference in the spectra shown in (a) and the specific extinction spectrum of aeCP597.
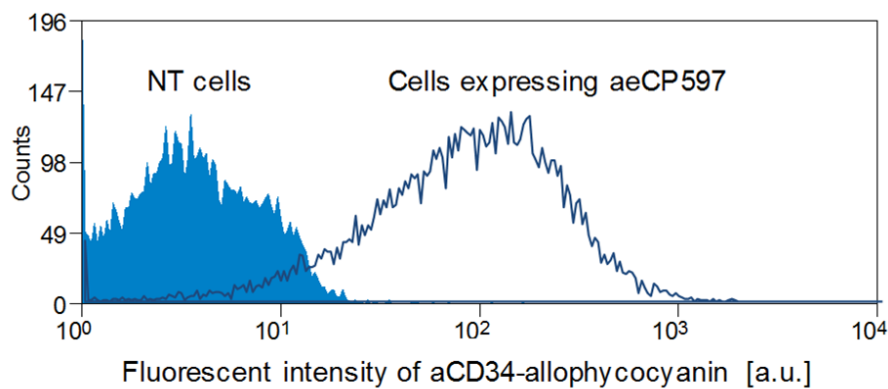

Fig. 7. Histogram of a fluorescence activated cell sorting (FACS) analysis of the expression levels of the CD34 surface protein, which was co-expressed with aeCP597, in normal type (NT) and transduced K562 cells.

4. Discussion

In this study, it was observed that the photoacoustic characteristics of fluorescent proteins and chromoproteins differed significantly. As Fig. 4 shows, the photoacoustic generation efficiency of the fluorescent proteins was found to be significantly less than that of the chromoproteins. This is in part because a proportion of the absorbed optical energy is converted to a fluorescent emission rather than thermal energy. However, the absorption-normalised spectra suggest that the reduction in generation efficiency is significantly greater than would be expected by this mechanism alone. Ground state depopulation [28] due to the relatively long electronic relaxation times (nanoseconds) of many fluorescent proteins [13], [14,29] may be responsible for the lower generation efficiency. It occurs when a fraction of the fluorescent molecules is promoted to an excited state, leaving fewer molecules to facilitate ground state absorption. As a consequence, the early arriving photons of a nanosecond photoacoustic excitation pulse would encounter proteins in the ground state and thus be absorbed. By contrast, later arriving photons within the same pulse would also encounter proteins in the excited state and not be absorbed. The net effect is to reduce the nominal absorption coefficient at the excitation wavelength, and therefore the photoacoustic signal amplitude. Chromoproteins, by contrast, do not fluoresce and are therefore likely to exhibit short, vibrational relaxations on a picosecond timescale [30]. This reduces the likelihood of ground state depopulation during a nanosecond excitation pulse and thus results in more

efficient thermalization and photoacoustic signal generation. This explanation is consistent with the absorption normalized photoacoustic spectra in Fig. 4 which show greater signal amplitudes produced by the chromoproteins than fluorescent proteins. Ground state depopulation may also explain the difference in shape between the photoacoustic and optical absorption spectra of fluorescent proteins (Fig. 2). At wavelengths away from the peak absorption, the likelihood that a photon is absorbed is low. Early arriving photons during an excitation pulse will therefore only excite a small proportion of the molecules, leaving sufficient molecules for absorption by later arriving photons. Under these circumstances, the photoacoustic spectrum agrees reasonably well with the optical absorption spectrum. At wavelengths nearer the absorption peak, the likelihood of absorption is much greater, leading to fewer ground state molecules available to absorb late arriving photons. Ground state depopulation is therefore more likely to occur at wavelengths around the absorption peak, resulting in reduced photoacoustic signal amplitude and hence a discrepancy with the optical absorption spectrum. By contrast, chromoproteins show good agreement between the shapes of the corresponding photoacoustic and optical absorption spectra due to their fast non-radiative electronic relaxation times, which inhibits ground state depopulation.

Another consequence of the long relaxation times of fluorescent proteins is oxidative photobleaching [31]. Long relaxation times increase the likelihood of electronic transitions via the triplet state [32], which is associated with even longer, millisecond electronic relaxations. This in turn increases the likelihood of producing highly reactive singlet oxygen that can permanently destroy the fluorophore. The different photobleaching rates of the various fluorescent proteins investigated here may be due to differences in the likelihood with which triplet states can occur in each protein. mRaspberry, for example, exhibited the fastest photobleaching with a 60% reduction in photoacoustic signal amplitude after exposure to 15000 nanosecond laser pulses, while most other fluorescent proteins showed a reduction in signal amplitude ranging from 50% to 30% within 35000 pulses. This is in qualitative agreement with reported fluorescence photobleaching caused by high intensity illumination [17,33,34,8]. Interestingly, E2 Crimson FP showed no signs of photobleaching. While there is evidence of biphasic bleaching in E2 Crimson FP [8], this was not observed in this study. A possible reason for this could be the differences in average radiant power. For the photoacoustic measurements the average radiant power was orders of magnitude lower than those used in the experiments performed by Strack et al. By contrast, chromoproteins, owing to their fast relaxation times, are much less likely to relax via the triplet state and therefore exhibit less photobleaching. This explanation is consistent with the results of this study, which show that fluorescent proteins tend to bleach much faster than chromoproteins. cjBlue and aeCP597 maintained 90% of the photoacoustic signal amplitude for over 35000 laser pulses, while E2 Crimson NF showed no signs of bleaching.

The potential application of chromoproteins as reporter genes in mammalian cells was demonstrated by expressing aeCP597 in human leukemia cells (K562). While the difference spectrum (Fig. 6(a)) clearly showed the presence of the reporter gene, the relatively low signal amplitude generated by the labelled cells illustrates one of the challenges for *in vivo* applications of this labelling strategy in mammalian organisms. If the expression level and therefore the intracellular concentration of aeCP597 is low, only a small increase in photoacoustic signal amplitude compared to the background will be detected. It may then be challenging to visualize such small changes in the presence of other, more abundant tissue chromophores, such as oxy- and deoxyhaemoglobin. Multiwavelength spectroscopic methods for reconstructing chromophore distributions from photoacoustic data, such as model-based inversion schemes [35,36], may therefore be required. The low expression levels also suggest that further optimization may be required. This would not be surprising since chromoproteins, such as aeCP597 and cjBlue, have not been optimized to function as genetic reporters in mammalian cells. For example, the green fluorescent protein commonly used today underwent many years of optimization [37]. It is feasible that chromoproteins may require a similar development program to yield biocompatible genetic labels with high expression levels and low toxicity.

5. Conclusion

Six commonly used fluorescent proteins (dsRed, mCherry, mNeptune, mRaspberry, AQ143, E2 Crimson) and three non-fluorescent chromoproteins (aeCP597, cjBlue and E2 Crimson NF) were synthesized and their photoacoustic spectra, signal generation efficiency and photostability measured. With the exception of E2 Crimson, all of the fluorescent proteins exhibited significant discrepancies between their photoacoustic and optical absorption spectra, low photoacoustic generation efficiency and poor photostability compared to the chromoproteins. Low photoacoustic signal generation efficiency and photobleaching are clearly disadvantageous. They lead to diminished image contrast whilst differences in the photoacoustic and absorption spectra would adversely affect the accuracy of quantitative spectroscopic and spectral unmixing imaging approaches which tend to rely on photostable chromophores and accurate a priori knowledge of their specific extinction spectra. Compared to the fluorescent proteins, the chromoproteins were found to be significantly more photostable and exhibit higher photoacoustic generation efficiency, the latter being a consequence of the absence of ground state depopulation and fluorescent emission. The photoacoustic spectra obtained in chromoproteins also agreed well with those of the corresponding optical absorption spectra. Furthermore, this study has provided evidence that photostable chromoproteins may be created from existing fluorescent proteins through genetic modification. This is evidenced by the non-fluorescent mutant E2 Crimson NF which showed increased absorption, and hence greater photoacoustic signal amplitudes, and good agreement between the photoacoustic spectra and the optical absorption spectrum compared to its fluorescent counterpart. In addition, we have demonstrated the expression of a chromoprotein (aeCP597) by mammalian cells. These results suggest that chromoproteins are an interesting option for the genetic labelling of mammalian cells in molecular photoacoustic imaging applications.